# EFFICIENT IMPLEMENTATION OF ADAPTIVE FIR-IFIR FILTERS USING THE LMS ALGORITHM

*Eduardo L. O. Batista, Orlando J. Tobias, and Rui Seara*

LINSE – Circuits and Signal Processing Laboratory
Department of Electrical Engineering
Federal University of Santa Catarina
88040-900 – Florianópolis – SC - Brazil
E-mails: {dudu, orlando, seara}@linse.ufsc.br

**ABSTRACT**

*This paper presents an approach for effectively implementing adaptive FIR-IFIR filters using the LMS algorithm. The motivation of such an approach is to use IFIR filters with removed boundary effect aiming to eliminate the loss of performance arisen from the FIR-IFIR combination for echo cancellation applications. Thereby, an algorithm with a better trade-off between performance and computational complexity is obtained as compared with other FIR-IFIR approaches. Numerical simulation results are presented attesting the effectiveness of the obtained algorithm.*

## 1. INTRODUCTION

The interpolated FIR (IFIR) filter is a reduced-complexity FIR implementation especially effective to realize FIR filters with impulse responses presenting smooth and predictable characteristics [1]. The low computational complexity of IFIR filters is obtained by implementing an FIR filter using a cascade structure composed of a sparse FIR filter, with reduced number of coefficients, and an interpolator. Such a reduced number of coefficients is particularly interesting for adaptive applications wherein, besides the filtering operation, the filter coefficients are updated at each iteration. In this context, a large variety of adaptive implementations of IFIR filters have been considered for different applications, such as active noise control [2], [3], audio processing in digital hearing aids [4], and interference suppression in CDMA systems [5]. Hybrid structures comprising FIR and IFIR filters have also been considered successfully for some other applications, such as echo cancelling in DSL systems [6]-[8] as well as echo and near-end crosstalk (NEXT) cancelling in 10GBASE-T Ethernet systems [9]. The effectiveness of such hybrid FIR-IFIR approaches arises from the characteristics of the echo and NEXT responses discussed in [6]-[9]. For instance, the typical echo response of some DSL systems exhibits a short and rapidly changing head section along with a long and slowly decaying tail segment, as illustrated in Figure 1 [6], [7]. Such a tail segment with smooth characteristics can be effectively modeled using an IFIR filter aiming to cancel the corresponding echo using less computational resources, whereas a conventional FIR filter is required to deal with the irregular head section. Additionally, for the cases described in [8], the tail segment can be split into smaller segments to allow the use of multiple IFIR echo cancellers with different sparseness characteristics. In the case of the echo and NEXT cancelling in 10GBASE-T Ethernet systems, described in [9], responses with characteristics comparable to those of the response shown in Figure 1 are observed. As a result, FIR-IFIR as well as three-stage IFIR-FIR-IFIR filters are considered.

The hybrid FIR-IFIR structure has been originally proposed in [6], focusing exclusively on the use of the IFIR part of the structure for cancelling the tail echo in DSL systems. However, the difficulties arisen from simultaneously using an FIR and an IFIR filter, for cancelling, respectively, the head and the tail echo, are not discussed in [6]. The most important among such difficulties is a distortion that arises from the FIR-IFIR impulse response as a consequence of an undesirable characteristic of ramp shape observed in the initial part of the IFIR impulse response [7]. Therefore, the tail echo is not cancelled properly and the performance of the complete FIR-IFIR echo canceller is poor. Aiming to solve the implementation issues neglected in [6], another approach to implement FIR-IFIR filters is presented in [7]. In this case, the length of the FIR impulse response is increased to produce an overlapping with the beginning of the IFIR impulse response. Thus, the FIR filter compensates for the distortion caused by the IFIR filter and a better performance is obtained. However, the cost to attain such a performance is an increase in computational load mainly due to the memory-size increase of the FIR filter. In the case of the FIR-IFIR echo and NEXT cancellers from [8] and [9], the difficulties arisen from the FIR-IFIR association are handled as in [6] and [7].

Contributing in this scope, a new approach for implementing FIR-IFIR filters is proposed. Such an approach is based on removing the undesirable initial part (of the IFIR impulse response) instead of compensating it increasing the memory size of the FIR part. By doing so, new procedures for implementing IFIR filters are developed considering the boundary effect removal techniques described in [10] and [11]. Such procedures are designed in line with the FIR-IFIR applications, resulting in IFIR implementations with smaller computational complexity than those from [10] and [11]. With no loss of generality, this paper is focused on the two-stage FIR-IFIR structures introduced in [6] and [7]. The application of the results obtained for the FIR-IFIR structures presented in [8] and [9] is straightforward and briefly described.

This paper is organized as follows. In Section 2, the FIR-IFIR approaches are described, focusing on the role of the boundary effect. In Section 3, a novel approach for implementing FIR-IFIR filters with removed boundary effect is presented and its computational cost is reported. Numerical simulation results are presented in Section 4, aiming to attest the effectiveness of the proposed approach. Finally, Section 5 presents the conclusions of this research work.

This work was supported in part by the National Council for Scientific and Technological Development (CNPq).

 ISSN 2076-1465 

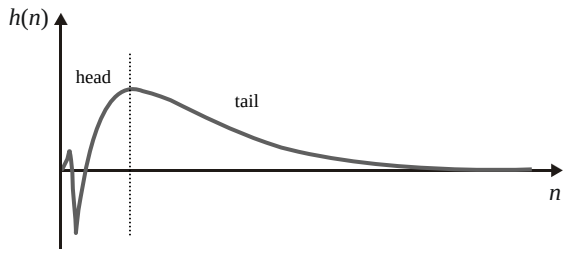


Figure 1 – Typical echo response in DSL systems.

## 2. FIR-IFIR STRUCTURES

The block diagram of an FIR-IFIR structure is presented in Figure 2 [6], [7]. In this figure, $\mathbf{w}_h$ represents the FIR filter and $\mathbf{w}_t$, the IFIR filter. Variables $x(n)$ and $y(n)$ denote, respectively, the input and output signals, and $z^{-D}$, a delay of $D$ samples. The latter is used to align the filter responses by enforcing the beginning of the response of $\mathbf{w}_t$ at the end of the response of $\mathbf{w}_h$. The choice of such a delay parameter is a function of the specific application characteristic.

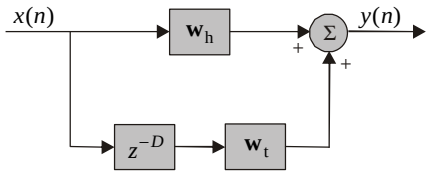


Figure 2 – Block diagram of an FIR-IFIR structure.

As previously mentioned, the FIR-IFIR structure has been originally proposed in [6] focusing on the behavior and performance of the IFIR part of the structure (IFIR filter $\mathbf{w}_t$). Such a filter is composed of an interpolator $\mathbf{g}$ cascaded with a sparse filter $\mathbf{w}_{ts}$ [6], [10]. The interpolator $\mathbf{g}$ has a memory size $M$ and a coefficient vector given by

$$\mathbf{g} = [g(0)\ \ g(1)\ \cdots\ g(M)]^{\mathrm{T}}. \tag{1}$$

The sparse filter $\mathbf{w}_{ts}$ has a memory size $N$ and the following coefficient vector:

$$\mathbf{w}_{ts} = \{w_t(0)\ 0\ \cdots\ w_t(L)\ 0\ \cdots\ w_t(2L)\ 0\ \cdots\ w_t[(N_{ts}-1)L]\ 0\ \cdots 0\}^{\mathrm{T}} \tag{2}$$

where $N_{ts} = [(N-D-1)/L]+1$ is the number of nonzero coefficients in $\mathbf{w}_{ts}$ and $L$, the interpolation or sparseness factor [10]. The memory size $M$ of the interpolator is usually given as a function of the interpolation factor [10]. Thus,

$$M(L) = 2L-1. \tag{3}$$

The equivalent coefficient vector of the IFIR filter $\mathbf{w}_t$, which corresponds to its impulse response, is given by [10]

$$\mathbf{w}_t = \mathbf{G}\mathbf{w}_{ts} \tag{4}$$

where

$$\mathbf{G} = \begin{bmatrix} g(0) & 0 & 0 & \cdots & 0 \\ g(1) & g(0) & 0 & \cdots & 0 \\ g(2) & g(1) & g(0) & \cdots & 0 \\ \vdots & \vdots & \vdots & \ddots & \vdots \\ g(M-1) & g(M-2) & g(M-3) & \cdots & g(0) \\ 0 & g(M-1) & g(M-2) & \cdots & g(1) \\ 0 & 0 & g(M-1) & \cdots & g(2) \\ \vdots & \vdots & \vdots & \ddots & \vdots \\ 0 & 0 & 0 & \cdots & g(M-1) \end{bmatrix} \tag{5}$$

is a convolution matrix with dimension $N+M-1\times N$ formed from $\mathbf{g}$ [10]. For instance, considering a case with $N=7$ and $L=2$, one has $M=3$, $\mathbf{g}=[g(0)\ g(1)\ g(2)]^{\mathrm{T}}$, $\mathbf{w}_{ts}=[w_t(0)\ 0\ w_t(2)\ 0\ w_t(4)\ 0\ w_t(6)]^{\mathrm{T}}$ and an equivalent coefficient vector given by

$$\begin{aligned}\mathbf{w}_t = \{ & g(0)w_t(0)\ \ g(1)w_t(0)\ \ [g(2)w_t(0)+g(0)w_t(2)] \\ & g(1)w_t(2)\ \ [g(2)w_t(2)+g(0)w_t(4)]\ \ g(1)w_t(4) \\ & [g(2)w_t(4)+g(0)w_t(6)]\ \ g(1)w_t(6)\ \ g(2)w_t(6)\}^{\mathrm{T}}.\end{aligned} \tag{6}$$

Now, considering the use of a linear interpolator with $\mathbf{g}=[0.5\ 1\ 0.5]^{\mathrm{T}}$, (6) is rewritten as

$$\begin{aligned}\mathbf{w}_t = [&\underline{0.5w_t(0)}\ w_t(0)\ \boxed{0.5w_t(0)+0.5w_t(2)}\ w_t(2)\ \boxed{0{,}5w_t(2)+0{,}5w_t(4)} \\ & w_t(4)\ \boxed{0.5w_t(4)+0.5w_t(6)}\ \ w_t(6)\ \ \underline{0.5w_t(6)}]^{\mathrm{T}}.\end{aligned} \tag{7}$$

By comparing (2) and (7), one can note that [10], [11]: (i) the coefficients from the sparse filter $\mathbf{w}_{ts}$ are replicated in $\mathbf{w}_t$; (ii) the zeroed coefficients in $\mathbf{w}_{ts}$ are recreated in $\mathbf{w}_t$ (boxed ones); and (iii) new coefficients (underlined) arise as a boundary effect. Due to such an effect, the impulse response of an IFIR filter exhibits transient responses decaying to zero at the beginning and at the end of the equivalent coefficient vector $\mathbf{w}_t$, as described in [7]. This characteristic becomes evident as an arbitrary sparse coefficient vector $\mathbf{w}_{ts}=[0.5\ 0\ 0.38\ 0\ 0.4\ 0\ 0.45]^{\mathrm{T}}$ is applied in (7). Thereby, one obtains a vector whose coefficients are illustrated in Figure 3, with the boundary effect highlighted through dashed lines. Such a decaying-to-zero characteristic of the boundary effect plays an important role when FIR and IFIR filters are associated, aiming to obtain FIR-IFIR structures. For instance, by using these structures for modeling the DSL echo response shown in Figure 1, the impulse response illustrated in Figure 4 is obtained. From this figure, one observes a significant mismatch between the echo response being modeled (gray line) and those obtained using the FIR (dotted line) and IFIR (dashed line) filters. As a consequence, a poor performance is obtained as using an FIR-IFIR echo canceller. Another approach for implementing FIR-IFIR filters aiming to overcome the drawbacks caused by the boundary effect is presented in [7]. Such an approach is based on increasing the memory size of the FIR filter for overlapping its impulse response with the part of the IFIR response corresponding to the boundary effect, as illustrated in Figure 5. Thus, some coefficients of the FIR filter are used to offset the distortion caused by the boundary effect in the FIR-IFIR response. Despite the very good performance obtained by using the FIR-IFIR approach from [7], an important increase in the computational burden is verified mainly due to the memory-size increase of the FIR filter. Moreover, from the results presented in [7], one observes that the memory size of the interpolator must also be increased to ensure a satisfactory performance of the algorithm.

For instance, in the case with an interpolation factor $L = 4$, an interpolator with 23 coefficients must be used, whereas only 7 interpolator coefficients would be usually required [see (3)]. Such an increase in memory size of the interpolator also implies an increase in computational burden. In addition, a reduction in the convergence speed of the adaptive algorithm due to the overlapping of the FIR and IFIR impulse responses is verified in [7], being such a reduction mitigated by setting some coefficients of the FIR filter to zero in the overlapping region [7]. In [8] and [9], other FIR-IFIR structures are introduced based on interesting strategies for reducing the computational burden in some specific applications. Concerning the distortion caused by the boundary effect, both these works adopt approaches similar to those presented in [6] and [7].

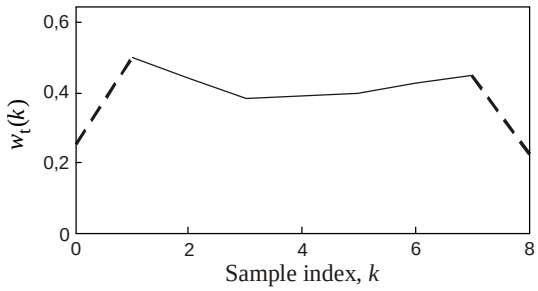


Figure 3 – Impulse response of an IFIR filter with the boundary effect highlighted using dashed lines.

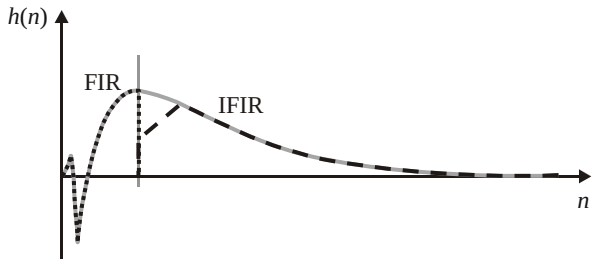


Figure 4 – Impulse response of the FIR-IFIR structure proposed in [6].

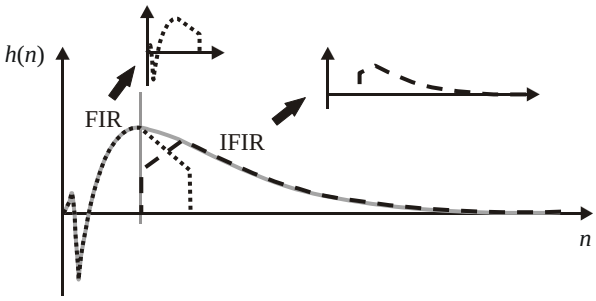


Figure 5 – Impulse response of the FIR-IFIR structure proposed in [7].

### 3. FIR-BIFIR APPROACH

Aiming to eliminate the distortion caused by the IFIR boundary effect in FIR-IFIR structures without increasing the computational burden, a novel approach for implementing FIR-IFIR filters is proposed. The idea here is to consider the particular characteristics of the applications of FIR-IFIR filters to develop new IFIR implementations based on IFIR filters with removed boundary effect [10], [11]. For instance, one important characteristic of the DSL echo responses, described in [6] and [7], is that the tail end always decays to zero (see Figure 1). As a consequence, the IFIR boundary effect at the end of the filter response does not present an important influence on modeling the echo response, which can be observed in Figures 4 and 5. Thus, the removal of the boundary effect is only required at the beginning of the IFIR response. With this aim, an IFIR implementation with removed boundary effect (BIFIR) is developed by modifying the procedure described in [10]. Thereby, one has a coefficient vector as in (2) and an input vector given by

$$\tilde{\mathbf{x}}'_{\mathrm{tb}}(n) = \mathbf{G}^{\mathrm{T}}\mathbf{T}_{\mathrm{b}}^{\mathrm{T}}\mathbf{x}_{\mathrm{t}}(n) \tag{8}$$

where $\mathbf{G}$ is given by (5), the modified transformation matrix $\mathbf{T}_{\mathrm{b}}$ is defined as

$$\mathbf{T}_{\mathrm{b}} = \begin{bmatrix} \underbrace{\begin{matrix} 0 & \cdots & 0 \\ 0 & \cdots & 0 \\ 0 & \cdots & 0 \\ 0 & \cdots & 0 \end{matrix}}_{L-1 \text{ columns}} & \underbrace{\begin{matrix} 1 & 0 & \cdots & 0 \\ 0 & 1 & \cdots & 0 \\ \vdots & \vdots & \ddots & \vdots \\ 0 & 0 & \cdots & 1 \end{matrix}}_{N+L-1 \text{ columns}} \end{bmatrix} \tag{9}$$

and the input vector $\mathbf{x}_{\mathrm{t}}(n)$ is given by

$$\begin{aligned} \mathbf{x}_{\mathrm{t}}(n) = [&x(n-D)\ \ x(n-D-1) \\ &x(n-D-2)\ \cdots\ x(n-N-L-D+2)]^{\mathrm{T}}. \end{aligned} \tag{10}$$

From (2) and (8), the input-output relationship of the BIFIR filter is written as

$$y_{\mathrm{t}}(n) = \mathbf{w}_{\mathrm{ts}}^{\mathrm{T}}\tilde{\mathbf{x}}'_{\mathrm{tb}}(n). \tag{11}$$

Now, since the BIFIR filter no longer presents a boundary effect, the memory of the FIR filter does not need to be increased to compensate for such effect as in [7]. Thus, the memory size of the FIR filter is now equal to the delay $D$ and its coefficient vector is then given by

$$\mathbf{w}_{\mathrm{h}} = [w_{\mathrm{h}}(0)\ \ w_{\mathrm{h}}(1)\ \ w_{\mathrm{h}}(2)\ \cdots w_{\mathrm{h}}(D-1)]^{\mathrm{T}}. \tag{12}$$

Moreover, the corresponding input vector is

$$\mathbf{x}_{\mathrm{h}}(n) = [x(n)\ \ x(n-1)\ \ x(n-2)\ \cdots\ x(n-D+1)]^{\mathrm{T}} \tag{13}$$

which results in the following input-output relationship:

$$y_{\mathrm{h}}(n) = \mathbf{w}_{\mathrm{h}}^{\mathrm{T}}\mathbf{x}_{\mathrm{h}}(n). \tag{14}$$

The proposed FIR-IFIR implementation, comprising FIR filters and IFIR ones with removed boundary effect (BIFIR), is termed here FIR-BIFIR and its impulse response, in the context of a DSL echo cancellation problem, is illustrated in Figure 6.

In adaptive applications of FIR-IFIR filters, due to computational complexity constraints, the LMS algorithm [12] is usually considered for coefficient updating. Thus, the LMS update equations for an FIR-BIFIR adaptive filter are given by

$$\mathbf{w}_{\mathrm{h}}(n+1) = \mathbf{w}_{\mathrm{h}}(n) + 2\mu_{\mathrm{h}}e(n)\mathbf{x}_{\mathrm{h}}(n) \tag{15}$$

and [13]

$$\mathbf{w}_{\mathrm{ts}}(n+1) = \mathbf{P}\mathbf{w}_{\mathrm{ts}}(n) + 2\mu_{\mathrm{t}}e(n)\mathbf{P}\tilde{\mathbf{x}}'_{\mathrm{tb}}(n) \tag{16}$$

where $\mu_{\mathrm{h}}$ and $\mu_{\mathrm{t}}$ are the step-size parameters and

$$e(n) = d(n) - y(n) = d(n) - y_{\mathrm{h}}(n) - y_{\mathrm{t}}(n) \tag{17}$$

is the error signal with $d(n)$ denoting the signal with echo. In (16), $\mathbf{P}$ denotes a projection matrix [13] enforcing the sparse coefficient vector $\mathbf{w}_{\mathrm{ts}}(n)$ to maintain its sparseness after each update.

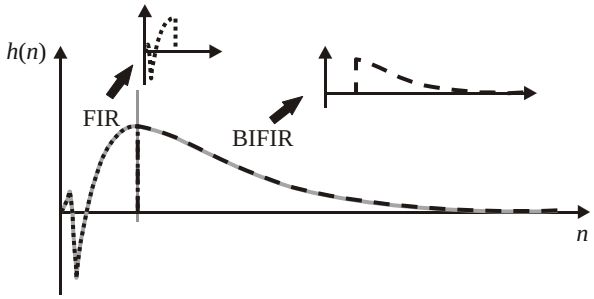


Figure 6 – Impulse response of the proposed FIR-BIFIR structure.

The FIR-BIFIR approach proposed here can also be applied to the FIR-IFIR structures presented in [8] and [9]. With this aim, one needs to take into account the parts of the echo response that decay to zero aiming to develop a well suited BIFIR implementation similar to that previously presented. For instance, in the case of the echo canceller presented in [9], an IFIR filter is used to model a part of the echo response whose initial segment decays to zero. In this case, the boundary effect must be removed only at the end part of the IFIR response. Thus, considering a memory size $N$ and an interpolation factor $L$, the resulting BIFIR filter has a coefficient vector given by (2) and its input vector is

$$\tilde{\mathbf{x}}'_{\mathrm{te}}(n) = \mathbf{G}^{\mathrm{T}}\mathbf{T}_{\mathrm{e}}^{\mathrm{T}}\mathbf{x}_{\mathrm{t}}(n) \tag{18}$$

where $\mathbf{G}$ is given in (5), $\mathbf{x}_{\mathrm{t}}(n)$ in (10), and $\mathbf{T}_{\mathrm{e}}$ is defined as

$$\mathbf{T}_{\mathrm{e}} = \left[\begin{array}{cccc|ccc} 1 & 0 & \cdots & 0 & 0 & \cdots & 0 \\ 0 & 1 & \cdots & 0 & 0 & \cdots & 0 \\ \vdots & \vdots & \ddots & \vdots & 0 & \cdots & 0 \\ 0 & 0 & \cdots & 1 & 0 & \cdots & 0 \end{array}\right]. \tag{19}$$

$\underbrace{\qquad\qquad\qquad}_{N+L-1 \text{ columns}}$ $\underbrace{\qquad\qquad}_{L-1 \text{ columns}}$

For this case, the LMS update is performed similarly to (16).

### 3.1. Computational Complexity

As discussed in [10], the BIFIR implementation results in an increase of $2L-2$ operations per sample as compared with the conventional IFIR one. However, in the modified BIFIR implementation developed here, only the boundary effect either at the beginning or at the end of the filter response is removed. As a result, $2L-2$ fewer operations per sample are required and the computational cost becomes the same as for implementing the conventional IFIR filter. The computational complexity required to implement an FIR-BIFIR filter adapted by the LMS algorithm using (15) and (16) (in terms of the number of operations per sample) is presented in Table 1. With the purpose of comparing the FIR-BIFIR implementation with the other FIR-IFIR ones in terms of computational burden, we consider here the setup used in [7] to obtain the simulation results. Thus, one has an FIR-IFIR structure with $N=250$, $L=4$, $D=31$, an FIR filter with 50 coefficients and an interpolator with 23 coefficients. For the FIR-BIFIR filter, we consider $N=250$, $L=4$ and $D=31$, which results in an FIR filter with $D=31$ coefficients and an interpolator with $M=7$ coefficients. Table 2 presents (for the considered case) a comparison of complexity between the conventional FIR, FIR-IFIR from [6], FIR-IFIR from [7], and the proposed FIR-BIFIR implementation. From this table, we verify a considerable reduction of complexity in favor of the FIR-IFIR approaches in comparison with the FIR filter. In addition, the proposed FIR-BIFIR approach presents the same computational complexity as the FIR-IFIR from [6] and a complexity reduction of almost 20% in comparison with the FIR-IFIR from [7].

TABLE 1
NUMBER OF OPERATIONS PER SAMPLE REQUIRED FOR IMPLEMENTING A FIR-BIFIR FILTER ADAPTED USING THE LMS ALGORITHM

| | FIR filter $\mathbf{w}_{\mathrm{h}}$ | | BIFIR filter $\mathbf{w}_{\mathrm{t}}$ | |
|---|---|---|---|---|
| | Filtering | Update | Filtering | Update |
| Multiplications | $D$ | $D$ | $M+N_{\mathrm{ts}}$ | $N_{\mathrm{ts}}$ |
| Sums | $D-1$ | $D$ | $M+N_{\mathrm{ts}}-2$ | $N_{\mathrm{ts}}$ |

TABLE 2
COMPLEXITY COMPARISON BETWEEN FIR, FIR-IFIR AND FIR-BIFIR FILTERS WITH $N=250$, $L=4$, AND $D=31$

| | Operations per sample | Relative percentages | |
|---|---|---|---|
| FIR | 999 | **100%** | |
| FIR-IFIR [6] | 355 | 35.5% | |
| FIR-IFIR [7] | 443 | 44.3% | **100%** |
| FIR-BIFIR (proposed) | 355 | 35.5% | 80.1% |

## 4. SIMULATION RESULTS

Aiming at a performance evaluation of the FIR-BIFIR implementation as compared with the FIR-IFIR approaches from [6] and [7], numerical simulation results are now presented. Such FIR-IFIR implementations are applied aiming at an echo cancellation problem whose impulse response, shown in Figure 7, presents characteristics similar to the echo responses considered in [7]. The memory size, interpolation factors, and delay values are the same as in the previous section. The performance of the filters are evaluated in terms of the echo return loss enhancement (ERLE), defined as [7]

$$\mathrm{ERLE} = 10\log_{10}\frac{E[d^2(n)]}{E[e^2(n)]} \tag{20}$$

where $d(n)$ is the signal with echo and $e(n)$, the error signal with the echo canceled. The ERLE curves are obtained from Monte Carlo simulations (average of 100 runs). Similar to [7], the line code of the input signal is 16-PAM.

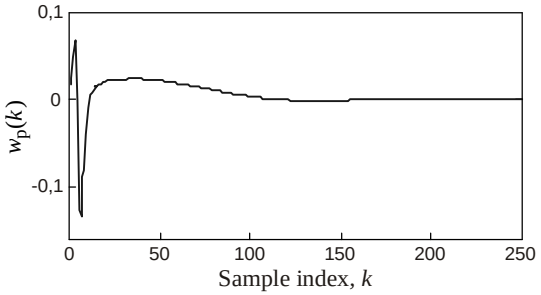


Figure 7 – Echo impulse response of a DSL system.

Simulation results are presented in Figure 8. Figure 8(a) shows the results obtained using the strategy for choosing the step-size parameter described in [7]. Thus, the total interval is divided into five stages and, for each stage, the step size is halved. The initial value for the step size is equal to a critical value $\mu_{\mathrm{crit}}$

that ensures the stability of the algorithm (experimentally obtained). In addition, Figure 8(b) presents the results obtained by using $\mu_{crit}$ during the whole interval, whereas Figure 8(c) shows the results obtained using different step-size values for the FIR and IFIR filters from the FIR-IFIR and FIR-BIFIR structures. From these results, we observe very good performance of the proposed FIR-BIFIR structure in comparison with the other FIR-IFIR structures.

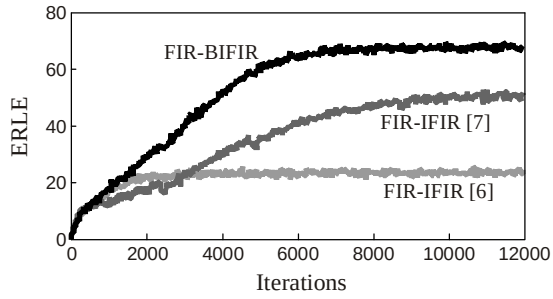


(a)

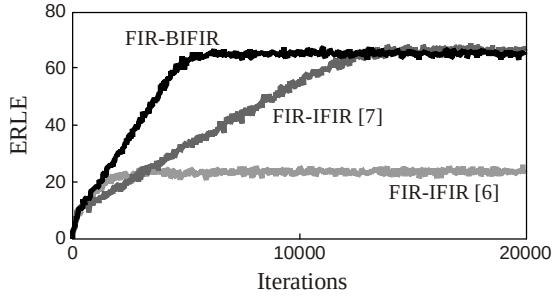


(b)

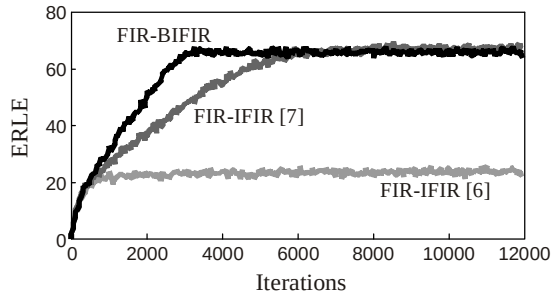


(c)

Figure 8 – ERLE Curves (average of 100 runs).

## 5. CONCLUSIONS

In this work, a novel approach for implementing FIR-IFIR filters has been presented. In comparison with the other FIR-IFIR approaches available in the literature, the proposed approach presents a better performance as well as a computational cost equal to that of the concurrent implementation having smaller computational cost. Numerical simulation results are presented corroborating the effectiveness of the proposed approach.

## REFERENCES


[1] Y. Neuvo, C. Y. Dong, and S. K. Mitra, "Interpolated finite impulse response digital filters," *IEEE Trans. Acoust., Speech, Signal Process.*, vol. 32, no. 3, pp. 563-570, Jun. 1984.

[2] S. Kuo and D. R. Morgan, *Active Noise Control Systems*. New York: John Wiley & Sons, 1996.

[3] K. Rajgopal and S. Venkataraman, "A delayless adaptive IFIR filterbank structure for wideband and narrowband active noise control," *Signal Processing*, vol. 86, no. 11, pp. 3421-3431, Nov. 2006.

[4] L. S. Nielsen and J. Sparso, "Designing asynchronous circuits for low power: An IFIR filter bank for a digital hearing aid," *Proceedings of the IEEE*, vol. 87, no. 2, pp. 268-281, Feb. 1999.

[5] R. de Lamare and R. Sampaio-Neto, "Reduced-rank interference suppression for DS-CDMA using adaptive interpolated FIR filters with adaptive interpolators," in *Proc. 15th IEEE Int. Symp. Personal, Indoor and Mobile Radio Comm.*, Barcelona, Spain, Sept. 2004, pp. 150-154.

[6] A. Abousaada, T. Aboulnasr, and W. Steenaart, "An echo tail canceller based on adaptive interpolated FIR filtering," *IEEE Trans. Circuits Syst. II, Analog Digit. Signal Process.*, vol. 39, no. 7, pp. 409-416, Jul. 1992.

[7] S.-S. Lin and W.-R. Wu, "A low-complexity adaptive echo canceller for xDSL Applications," *IEEE Trans. Signal Process.*, vol. 52, no. 5, pp. 1461-1465, May. 2004.

[8] C. Wu and A. Wu, "A novel cost-effective multi-path adaptive interpolated FIR (IFIR)-based echo canceller," in *Proc. IEEE Int. Symp. Circuits Syst. (ISCAS)*, Scottsdale, USA, May 2002, pp. V-453-V-456.

[9] Y. Chen, C. Zhan, and A. Wu, "Cost-effective echo and NEXT canceller designs for 10GBASE-T ethernet system," in *Proc. IEEE Int. Symp. Circuits Syst. (ISCAS)*, Seattle, USA, May 2008, pp. 3150-3153.

[10] E. L. O. Batista, O. J. Tobias, and R. Seara, "A fully adaptive IFIR filter with removed border effect," in *Proc. IEEE Int. Conf. Acoust., Speech, Signal Process. (ICASSP)*, Las Vegas, USA, Apr. 2008, pp. 3821-3824.

[11] E. L. O. Batista, O. J. Tobias, and R. Seara, "Border effect removal for IFIR and interpolated Volterra filters," in *Proc. IEEE Int. Conf. Acoust., Speech, Signal Process. (ICASSP)*, Honolulu, USA, vol. 3, Apr. 2007, pp. 1329-1332.

[12] B. Farhang-Boroujeny, *Adaptive Filters Theory and Applications*. New York: John Wiley & Sons, 1999.

[13] E. L. O. Batista, O. J. Tobias, and R. Seara, "A sparse-interpolated scheme for implementing adaptive Volterra filters," *IEEE Trans. Signal Process.*, to be published.